ORIGINAL RESEARCH

Imaging Characteristics of Schwannoma of the Cervical Sympathetic Chain: A Review of 12 Cases

G. Anil
T.Y. Tan

BACKGROUND AND PURPOSE: SCSCs are rare. This study reviews our experience with CT and MR imaging of SCSCs.

MATERIALS AND METHODS: We retrospectively reviewed the CT and MR imaging studies as well as clinical data of 12 patients (6 men, 6 women; mean age, 41 years; range, 27–55 years) with surgicopathologic evidence of SCSC, referred to our institution between January 1999 to October 2008. Images were evaluated with respect to the location, number, morphology, attenuation/signal intensity, enhancement characteristics, and patterns of mass effect of the schwannomas.

RESULTS: The schwannomas were solitary, well-circumscribed, and medial to the carotid sheath. Seven were hypoattenuated to skeletal muscle on CT with poor postcontrast enhancement, 4 were isoattenuated, and a single lesion showed intense heterogeneous enhancement. At MR imaging, they were heterogeneously bright on T2WI with intense inhomogeneous postgadolinium enhancement. The ICA was displaced anteriorly in 9 patients with a component of lateral displacement in 8 of these patients. The ICA was in a neutral position in 2 patients and posterolaterally displaced in 1 patient. A single patient demonstrated separation of the ICA and IJV. There was splaying of the carotid bifurcation in 4 patients.

CONCLUSIONS: We present the patterns of mass effect and the spectrum of CT and MR imaging characteristics of SCSC, including certain observations that are infrequently described in the published literature.

ABBREVIATIONS: ECA = external carotid artery; ICA = internal carotid artery; IJV = internal jugular vein; S = schwannoma; SCSC = schwannoma of the cervical sympathetic chain; T1WI = T1-weighted imaging; T2WI = T2-weighted imaging

Schwannoma is a benign slow-growing encapsulated nerve sheath tumor composed of Schwann cells in a collagenous matrix that can arise from any cranial, peripheral, or autonomic nerve in the body. Most extracranial schwannomas are found in the parapharyngeal space and are usually of vagal origin.[1,2] Meanwhile, an SCSC is a rare entity. Most of the published material on SCSC are either case reports or small series, recorded primarily in the surgical literature, with limited emphasis on imaging. This study was a review of our institutional experience with CT and MR imaging-based evaluation of this neoplasm, with emphasis on the imaging characteristics and patterns of mass effect. We present a spectrum of findings in patients with SCSC, including certain observations that are infrequently described in the literature published in the English language.

Materials and Methods

We retrospectively reviewed CT and MR imaging studies of 12 patients (6 men and 6 women; mean age, 41 years; range, 27–55 years) with SCSC, referred to our institution, a 900-bed Joint Commission International Accreditation–accredited multispecialty hospital, from January 1999 to October 2008. Ten patients presented with a lateral neck mass of variable duration (3 months to 6 years), while the tumor was incidentally detected in 2 of them. Besides the neck mass, there was Horner syndrome at presentation in 1 patient and dysphagia in 2 patients. Surgical and pathologic confirmation of the diagnosis was the inclusion criterion. In 11 patients, the nerve of origin was determined by direct visualization at surgery. In 1 patient, the sympathetic trunk was equivocal at surgery for the nerve of origin. However, this patient developed complete postoperative Horner syndrome; hence, she was included in this study. All the tumors were benign schwannomas based on the histopathology reports.

The contrast-enhanced CT or MR imaging or both were performed in our department or at the primary referring institution. Both CT and MR imaging were available for review in 5 patients, while only CT had been performed in 7 patients. Because these studies were performed at different points in time, at different institutions, and on different scanners, the imaging techniques varied. However, all the CT scans were postcontrast studies with z-axis coverage from the skull base to the arch of the aorta, performed on a spiral CT or multisection scanner. The section thickness and pitch were in the range of 3–5 mm and 1–1.5, respectively. The multidetector row CT studies were reconstructed at 3- to 5-mm thickness in both axial and coronal planes. The MR imaging studies included multiplanar images obtained on a 1T or 1.5T scanner. The minimum sequences included axial T1WI (TR, 200–700 ms; TE, 9–30 ms), T2WI (TR, 2000–4000 ms; TE, 80–120 ms), and coronal short tau inversion recovery imaging (TI, 120–150 ms). Postgadolinium images were obtained in at least 2 or-

Received November 22, 2009; accepted after revision March 8, 2010.

From the Department of Radiology, Changi General Hospital, Singapore.

Paper previously presented at: 34th Annual Meeting of European Society of Neuroradiology, September 17–20, 2009; Athens, Greece.

Please address correspondence to Gopinathan Anil, MD, Department of Radiology, Changi General Hospital, 2 Simei St 3, Singapore 529889; e-mail: ivyanil10@gmail.com

DOI 10.3174/ajnr.A2212

Fig 1. These postcontrast axial CT images of 3 different patients demonstrate the variable appearances of the SCSC with respect to their texture and attenuation. All of them are well-defined and round to oval with anterior (*A*) or anterolateral (*B* and *C*) displacement of the vessels in the carotid sheath. There is no separation of the IJV and ICA. *A*, The schwannoma is homogeneously hypoattenuated to the skeletal muscle, with almost no enhancement. *B*, The schwannoma is predominantly isattenuated with enhancement similar to that of the skeletal muscle. Internal heterogeneity is noted as an irregular poorly enhancing hypoattenuated area in its anteromedial quadrant. *C*, The schwannoma shows marked internal heterogeneity. Central areas are intensely enhancing, while the rest of the tumor is moderately or poorly enhancing.

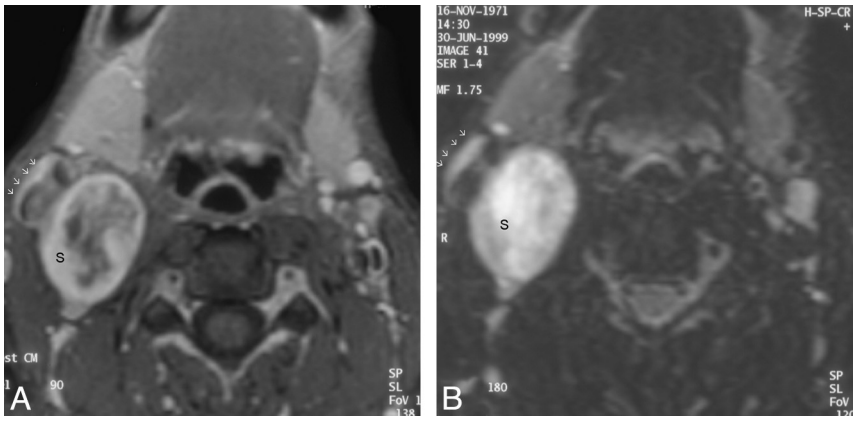

Fig 2. The schwannoma shows intense heterogeneous enhancement on the postgadolinium fat-saturated T1WI (*A*) and appears heterogeneously bright on the fat-saturated T2WI (*B*). The nonenhancing areas in the center of the mass correspond to the areas of fluid signal intensity seen in the T2WI. The entire carotid sheath (*arrows*) is displaced in an anterolateral direction.

thogonal planes. The section thicknesses varied from 3 to 5 mm; and intersection gap, from 1 to 2.5 mm. Additional sequences were available in some patients—that is, fat-saturated T2WI in 3 patients, 2D time-of-flight images with the protocol selected for the carotid arteries in 2 patients, and gradient-weighted images in 1 patient.

The images were reviewed by 2 radiologists, and findings were recorded by consensus. The scans were evaluated as to tumor location, relation to the vessels in the carotid space, patterns of mass effect on the adjoining fat planes and structures, attenuation/signal intensity, and enhancement pattern. The lesion margins (well-defined or ill-defined), shape (round-to-oval or irregular), size (long- and short-axis diameters measured on axial images), and number (single or multiple) were also noted. CT attenuation was compared with that of the adjoining skeletal muscles. Postcontrast enhancement was subjectively graded as poor, moderate, or intense. Enhancement similar to skeletal muscle was considered moderate; that less than skeletal muscle, as poor; and that approaching the attenuation of contrast in the vessels, as intense. The tumor was classified as being of high signal intensity on T2WI if it had signal intensity greater than that of fat and as being of low signal intensity on T1WI if it had signal intensity lower than that of muscle. Postgadolinium enhancement was compared with precontrast T1WI and was graded in the same manner as it was with CT. The tumor texture was recorded as heterogeneous or homogeneous in attenuation/signal intensity. On MR imaging, this was based on the appearance on T2WI.

Results

All tumors were well-circumscribed, solitary, of round to oval shape and located medial to the vessels of the carotid sheath. The average long-axis diameter of the tumor was 3.5 cm (range, 1.5–5 cm), and the average short-axis diameter was 2.6 cm (range, 1–4 cm).

At CT scanning, 7 patients had tumors that were hypoattenuated, with poor enhancement compared with adjoining skeletal muscles (Fig 1*A*). Four tumors were isoattenuated to skeletal muscle (Fig 1*B*), while there was intense heterogeneous enhancement in a single tumor (Fig 1*C*). Seven of them had a heterogeneous texture, while 5 were homogeneous on CT scans. At MR imaging, the tumors were of low-to-intermediate signal intensity on T1WI and heterogeneously hyperintense on T2WI and showed intense postgadolinium enhancement (Fig 2). There were no flow voids seen in any of the tumors. MR imaging demonstrated the internal heterogeneity better than CT. In the 4 patients who underwent both CT and MR imaging, we found that the delineation of the surrounding fat planes and the relationship with soft tissue and vascular structures as well as tumor texture were better demonstrated on the latter. The contrast-enhanced CT scans could provide the same information, though the structures were more obvious on MR imaging.

Nine of the 12 SCSCs straddled both the supra- and infrahyoid neck; however, the bulk of these tumors lay above the

Fig 3. The postcontrast axial CT image shows the SCSC as a hypoattenuated mass with poor enhancement. There is posterolateral displacement of the right ICA and IJV. This is unlike the anterior displacement of the ICA that is normally seen in carotid space masses (compare with the earlier figures). However, true to its carotid space location, there is anterior displacement of the fat in the prestyloid parapharyngeal space, and it displaces the visceral space medially.

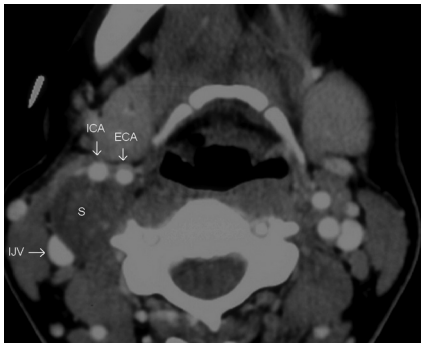

Fig 4. This postcontrast axial CT image demonstrates the separation of the right IJV and ICA by the SCSC. Tumors of the sympathetic chain usually displace the ICA and IJV together, without separating them. On imaging, it is almost impossible to distinguish the tumor in this image from a vagal schwannoma. Such a lesion may be considered as a caveat to the paradigm of Furukawa et al.[16]

level of the carotid bifurcation. Three of them were purely suprahyoid, located entirely above the level of carotid bifurcation. In 10 patients, the fat in the parapharyngeal space was displaced anteriorly, while the visceral space was displaced medially. Nine of the 12 tumors displaced the ICA in the anterior direction with 8 of them also displaying a component of lateral displacement (Figs 1 and 2). In 2 cases when the tumors were much smaller than average (measuring, 1.5 × 1 cm), the artery was in a neutral position compared with the contralateral side. In a single case, the ICA (along with the IJV) was displaced posterolaterally (Fig 3). The tumor separated the ICA from the IJV in 1 patient (Fig 4); the rest of the patients characteristically lacked such a separation of the vessels.

In 4 patients, the tumor splayed the ICA and ECA (Fig 5). In 3 of these 4 patients, the tumor separated the ICA and ECA along an anteroposterior axis (within 30° from the sagittal plane) with the ECA anterior to the tumor and the ICA posterior. In the remaining patient, the tumor separated the arteries in an oblique plane, once again with the ECA anterior to ICA. The ICA was posterior to the tumor in these 4 patients, but just 1 patient demonstrated posterior displacement of the artery compared with the contralateral side. The ICA was neutrally placed in 2 of these patients and was anterior to the contralateral side in the remaining patient. The ICA and ECA were either stretched about the schwannoma (in 2 patients), or they

Fig 5. In this postcontrast axial CT image, the schwannoma separates the ICA and ECA along a sagittal plane. The arteries are being splayed but not encased by the tumor, and there is <180° of contact between the tumor and the vessel. The ICA is posterior to the tumor; still, it is in a neutral position compared with the contralateral side. In this case, the tumor is probably too small to displace the arteries or adjoining fat planes.

coursed anterior and posterior to the tumor, just abutting it (2 patients). In all of these patients, there was <180° of contact between the tumor and the arteries. The schwannomas neither encased arteries nor filled the crotch of the carotid bifurcation.

Postoperative Horner syndrome was noted in all patients. In 10 patients it was partial and transient with gradual recovery. Two patients developed complete Horner syndrome. One partially recovered, while in the other patient, the syndrome persisted at 1 year after surgery.

Discussion

The cervical sympathetic trunk is located posteromedial to the carotid vessels as it runs longitudinally over the longus capitis and longus colli muscles, deep to the prevertebral fascia.[3] In 16.7% of cases, it can even pass within the wall of the carotid sheath.[4] In strict anatomic terms, the sympathetic chain is outside the carotid sheath, yet in practice, lesions arising from this structure are included in carotid space pathologies.[5] There are 3 ganglia in the cervical sympathetic chain. The superior one is the largest and most consistent in location, often found at the level of the carotid sinus, usually between the C2 and C4 levels. The middle sympathetic ganglion is the smallest and is located at a level where the inferior thyroid artery crosses the trunk (usually around C6). The inferior ganglion is variable in position, and it often fuses with the first thoracic ganglion to form the stellate ganglion.[3,4,6] The superior ganglion has a diameter of 5.3 (±0.6 mm), and the sympathetic chain at the level of C6 has a thickness of 3.3 (±0.6) mm.[3] Hence, these structures may be visualized in a healthy individual, though they are not always obvious due to the complex regional anatomy. This awareness can prevent a prominent normal ganglion from being misinterpreted as pathology. The normal ganglion is usually hypointense on T2WI, a finding that may help distinguish it from a schwannoma or enlarged retropharyngeal node.[7]

SCSCs are slow-growing tumors, often asymptomatic at presentation. The referral is usually initiated by the neck mass as seen in most of our patients. Vague symptoms like dysphagia and sore throat may be present. Features of nerve compression are rare because the cervical sympathetic trunk lies in a relatively loose fascial compartment and schwannomas, by na-

ture, are noninfiltrative. Hence, the incidence of Horner syndrome before excision is extremely rare, as seen in a single patient from this series.[8] Complete excision without major complications is possible with an extremely low recurrence rate. Postoperative Horner syndrome is common, but usually it is transient, with gradual recovery, as seen during this study.[8,9] Surgical excision is the treatment of choice, but slow growth and the noninvasive nature of SCSCs also allow an observational approach.

In the literature, schwannomas have been described as hypo-, iso-, or hyperattenuated (Fig 1), with variable texture (heterogeneous or homogeneous) and enhancement on CT.[10,11] The heterogeneity has been attributed to cystic degeneration, xanthomatous change, or areas of relative hypocellularity adjacent to densely cellular or collagenous regions.[12] More than half of the schwannomas (58%) encountered in this study had a heterogeneous texture; however, some of this may be due to patchy enhancement (there were no unenhanced images for comparison). Lack of information on the interval between image acquisition and contrast injection was among the drawbacks of this retrospective analysis. Still, in 2 patients, there was marked heterogeneity and obvious areas of cystic changes, which were supported by corresponding MR imaging findings. Schwannomas are hypovascular tumors, but if images are acquired beyond the first 60 seconds after the contrast injection, they can show marked enhancement due to pooling of contrast from poor venous drainage, simulating a hypervascular lesion.[2,13] The different patterns of contrast enhancement seen during this study can be explained by the aforementioned postcontrast enhancement dynamics. The MR imaging findings of low-to-intermediate signal intensity on T1WI, heterogeneous hyperintensity on T2WI, and intense heterogeneous postgadolinium enhancement (Fig 2) are consistent with the standard teachings on schwannomas.[2,11]

The target sign for schwannomas, described in the literature, was not seen in any patient from this study. Although typically described in the extremities, it may be seen elsewhere. The target appearance is mimicked by tumors with central areas of hypointensity and surrounding hyperintensity on T2WI axial images, due to an accumulation of the hypercellular Antoni type A bodies at the center with hypocellular Antoni type B bodies at the periphery.[14]

Our results regarding the average size, margin, appearance, and location within the lateral neck of SCSCs are concordant with those of the literature. The anterior displacement of parapharyngeal fat and the medial displacement of the visceral space (Fig 3), as demonstrated in most of the patients from this study, are typical of a carotid space lesion.[5,10] The anterior displacement of the ICA seen in 75% of our patients is comparable with the findings in earlier studies on nerve sheath tumors of the carotid space.[11,13] By virtue of the anatomic location of the sympathetic chain, posteromedial to the carotid sheath, SCSCs tend to displace the ICA and CCA in an anterior and lateral direction (Figs 1 and 2).[5]

In this study, approximately 67% (8 patients) showed this pattern of anterolateral displacement of the ICA. In 2 patients, the small tumor size presumably did not cause adequate mass effect; hence, the ICA was in a neutral position compared with the opposite side (Fig 5). Posterior displacement of the ICA by a carotid space schwannoma is rare,[11,15] as seen in just a single patient from this study (Fig 3). The vagus nerve runs between the IJV and ICA in the entire carotid sheath; hence vagal tumors tend to separate these vessels. The sympathetic chain is located posteromedial to both of these vessels; hence such a separation is not usually seen with SCSCs. Eleven tumors from this study complied with the above observation reported by Furukawa et al.[16] However in 1 patient, an SCSC was seen separating the IJV and ICA, with the former displaced posteriorly and the latter, anteriorly, making it difficult to distinguish it from a vagal tumor (Fig 4). A similar observation was reported earlier.[15]

According to Parsons,[17] the prevertebral and pretracheal layers of the deep cervical fascia, which form the carotid sheath, exist only as undifferentiated tissue with the consistency of loose cotton wool. This tissue is lax enough to permit independent movement of its contents and is not a restrictive sheath. With this outlook, one may speculate that a tumor arising from the sympathetic chain, from its posteromedial position with respect to the carotid sheath, can cause a standalone anterior displacement of the artery, separate from the vein. The more lateral location of the vein compared with the artery from the sympathetic chain may facilitate such an isolated displacement of the artery. In such an event, the tumor can grow in the plane between the vein and artery and cause their separation. The other probable mechanism could be a variation in the course of the sympathetic chain. Irrespective of the mechanism, this unusual finding of the splaying of the IJV and ICA by the SCSC may be added as a caveat to the paradigm of Furukawa et al.[16]

SCSCs can splay the ECA and ICA and mimic the "Lyre" sign, classically described for carotid body tumors (Fig 5).[18] As the carotid body tumor arises from the wall of the common carotid artery, it tends to completely fill the crotch of the bifurcation[2] and encase the ICA and ECA.[19] In our experience, schwannomas do not fill the crotch of the carotid bifurcation because we could identify the angle of the bifurcation in all 4 patients with SCSC splaying the carotid arteries. We found the SCSC merely separating the ICA and ECA as well as the arteries stretched about the tumor; yet the contact between them did not exceed 180° of the vessel circumference. This suggests that the SCSC splays the bifurcation but without encasing the arteries. Although the current sample size of 4 patients is too small to endorse this finding as a reliable sign, it may be explored in the future as a distinguishing feature from carotid body tumor.

Metastatic lymph nodes, paragangliomas, and vagal schwannomas are the usual differential diagnoses to be considered. Metastatic lymph nodes are often multiple, with a known primary, making the diagnosis easy.[2] However, a solitary metastatic node from an unknown primary cancer may be difficult to differentiate from a schwannoma in the absence of periadenitis or extranodal extension of disease. Paragangliomas show early arterial enhancement on CT; they are hypervascular lesions (while schwannomas are hypovascular) and show certain characteristic MR imaging appearances like scattered flow voids ("salt and pepper" appearance), that usually enable the appropriate diagnosis.[20] Their pattern of splaying the carotid bifurcation is also distinct from that of SCSC. On most occasions, separation of the IJV and ICA is useful to distinguish vagal and sympathetic chain schwannomas.[15,16]

Conclusions

In conclusion, we present the spectrum of CT and MR imaging findings of SCSCs. They tend to be well-circumscribed, solitary, round to oval, and medial to the vessels of the carotid sheath. On CT, they are mostly hypo- to isoattenuated with poor-to-moderate heterogeneous postcontrast enhancement. They are heterogeneously bright on T2WI with inhomogeneous but intense postgadolinium enhancement. They routinely displace the ICA anteriorly or anterolaterally, fat in the parapharyngeal space anteriorly, and the visceral space medially. However in small-sized tumors, these patterns of mass effect may not be seen. Occasionally, an SCSC may displace the ICA posteriorly. If the SCSC grows between the ICA and IJV, it is difficult to distinguish from a vagal schwannoma; however, this is a rare occurrence. When the SCSC splays the ICA and ECA, it neither fills the crotch of the carotid bifurcation nor encases the arteries. Knowledge of these imaging features can be useful in the differential diagnosis of lateral neck masses and in making a preoperative diagnosis of this rare neoplasm.

References

1. Malone JP, Lee WJ, Levin RJ. **Clinical characteristics and treatment outcome for nonvestibular schwannomas of the head and neck.** *Am J Otolaryngol* 2005;26:108–12
2. Som PM, Curtin HD. **Parapharyngeal space.** In: Som PM, Curtin HD, eds. *Head and Neck Imaging*. Vol 2. 3rd ed. St Louis: Mosby; 1996:915–51
3. Civelek E, Karasu A, Cansever T, et al. **Surgical anatomy of the cervical sympathetic trunk during anterolateral approach to cervical spine.** *Eur Spine J* 2008; 17:991–95. Epub 2008 Jun 12
4. Lyons AJ, Mills CC. **Anatomical variants of the cervical sympathetic chain to be considered during neck dissection.** *Br J Oral Maxillofac Surg* 1998;36: 180–82
5. Harnsberger HR, Osborn AG. **Differential diagnosis of head and neck lesions based on their space of origin. 1. The suprahyoid part of the neck.** *AJR Am J Roentgenol* 1991;157:147–54
6. Tubbs RS, Salter EG, Oakes WJ. **Anatomic landmarks for nerves of the neck: a Vade Mecum for neurosurgeons.** *Neurosurgery* 2005;56:256–60
7. Yuen HW, Goh CHK, Tan TY. **Enlarged cervical sympathetic ganglion: an unusual parapharyngeal space tumour.** *Singapore Med J* 2006;47:321–23
8. Wax MK, Shiley SG, Robinson JL, et al. **Cervical sympathetic chain schwannoma.** *Layrngoscope* 2004;114:2210–13
9. Hood RJ, Reibel JF, Jensen ME, et al. **Schwannoma of the cervical sympathetic chain.** *Ann Otol Rhinol Laryngol* 2000;109:48–51
10. Silver AJ, Mawad ME, Hilal SK, et al. **Computed tomography of the carotid space and related cervical spaces. Part II. Neurogenic tumors.** *Radiology* 1984;150:729–35
11. Som PM, Sacher M, Stollman AL, et al. **Common tumors of the parapharyngeal space: refined imaging diagnosis.** *Radiology* 1988;169:81–85
12. Cohen LM, Schwartz AM, Rockoff SD. **Benign schwannoma: pathological basis for CT inhomogeneities.** *AJR Am J Roentgenol* 1986;147:141–43
13. Som PM, Biller HF, Lawson W, et al. **Parapharyngeal space masses: an updated protocol based upon 104 cases.** *Radiology* 1984;153:149–56
14. Murphey MD, Smith WS, Smith SE, et al. **From the archives of the AFIP: imaging of musculoskeletal neurogenic tumors—radiologic-pathologic correlation.** *Radiographics* 1999;19:1253–80
15. Saito DM, Glastonbury CM, El Sayed IH, et al. **Parapharyngeal space schwannomas.** *Arch Otolaryngol Head Neck Surg* 2007;133:662–67
16. Furukawa M, Furukawa MK, Katoh K, et al. **Differentiation between schwannoma of the vagus nerve and schwannoma of the cervical sympathetic chain by imaging diagnosis.** *Laryngoscope* 1996;106:1548–52
17. Parsons FG. **On the carotid sheath and other fascial planes.** *J Anat Physiol* 1910;44:153–55
18. Wang CP, Hsiao JK, Ko JY. **Splaying of the carotid bifurcation caused by a cervical sympathetic chain schwannoma.** *Ann Otol Rhinol Laryngol* 2004;113: 696–99
19. Arya S, Rao V, Juvekar S, et al. **Carotid body tumors: objective criteria to predict the Shamblin group on MR imaging.** *AJNR Am J Neuroradiol* 2008;29: 1349–54. Epub 2008 Apr 16
20. Rao AB, Koeller KK, Adair CF. **Paragangliomas of the head and neck: radiologic-pathologic correlation.** *Radiographics* 1999;19:1605–32